論文 / 著書情報
Article / Book Information

Title	Power Consumption Comparison Between Mammal-Type and Reptile-Type Multi-Legged Robots During Static Walking
Authors	Shuhei Tsunoda, Hiroyuki Nabae, Koichi Suzumori, Gen Endo
Citation	Proceedings of the 2022 IEEE/SICE International Symposium on System Integration, , , pp. 459-466
Pub. date	2022, 1
Copyright	(c) 2022 IEEE. Personal use of this material is permitted. Permission from IEEE must be obtained for all other uses, in any current or future media, including reprinting/republishing this material for advertising or promotional purposes, creating new collective works, for resale or redistribution to servers or lists, or reuse of any copyrighted component of this work in other works.
DOI	http://dx.doi.org/10.1109/SII52469.2022.9708790
Note	This file is author (final) version.

Power Consumption Comparison Between Mammal-Type and Reptile-Type Multi-Legged Robots During Static Walking

Shuhei Tsunoda[1], Hiroyuki Nabae[1], Koichi Suzumori[1], and Gen Endo[1]

***Abstract*— The leg configurations of multi-legged robots are classified into mammal-type and reptile-type. However, few studies have quantitatively compared the two leg configurations. We compared the power consumed during static walking when the parameters of walking, such as body height and foot trajectory, are changed. These parameters were not investigated in previous studies. In addition, we compared the power consumption when the robots walked sideways and diagonally. The analysis results showed that regardless of the direction in which the robot walked, the reptile-type configuration is able to maintain low power consumption over a wide range of foot positions. Furthermore, the reptile-type configuration can reduce the power consumption by lowering the body height, which simultaneously achieves improved stability and a wider range of foot positions. We also found that, by increasing the reduction ratio of the second joint from the body, the reptile-type configuration can reduce the power consumption without significantly reducing the maximum walking speed. These results indicate that the reptile-type configuration is superior to the mammal-type configuration in terms of the power consumption during static walking. The results of this research would be meaningful for applications requiring stable walking even at low speed.**

I. INTRODUCTION

Walking robots can be used in uneven terrain environments where wheeled mobile machines are usually unable to enter, as they can discretely select the ground contact point. In addition, unlike crawler-type mobile machines, they are expected to play an active role in disaster sites because they are less likely to destroy unstable ground such as rubble, and they themselves can serve as a stable foundation in uneven or sloped environments. Among the various types of walking robots, multi-legged robots with four or more legs are stable and relatively easy to control because even if one leg is lifted off the ground during the walking cycle, the body can be supported by the remaining three or more legs.

Typical multi-legged robots include quadruped robots and hexapod robots. Quadruped robots can support their body with exactly three legs when one leg is lifted off the ground. This means that they have the minimum number of legs necessary to walk statically. Therefore, it can be said that quadruped robots balance the stability and simplicity of their structure. In contrast, hexapod robots have more complex structure, but they can maintain a larger support polygon. Furthermore, by moving three legs alternately, they can walk at a high speed with a duty ratio of 0.5 while maintaining static stability. They can also walk while grasping an object or performing another task using two legs.

[1]All authors are with the Department of Mechanical Engineering, Tokyo Institute of Technology, 2-12-1 Ookayama, Meguro-ku, Tokyo 152-8550, Japan tsunoda.s.ad@m.titech.ac.jp

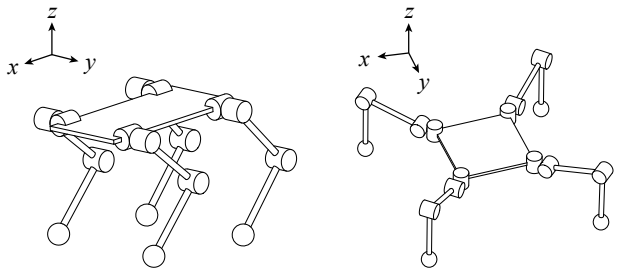

(a) Mammal-type (b) Reptile-type

Fig. 1. Schematics of two types of leg configurations for quadruped robots.

Based on their degrees of freedom arrangement, multi-legged robots can be roughly divided into mammal-type and reptile-type robots, as shown in Fig. 1. In the mammal-type configuration, the joints closest to the body rotate around the x-axis, which is the walking direction, and the knees bend back and forth. In the reptile-type configuration, the joints closest to the body rotate around the z-axis, which is the vertical direction, and the knees bend in various directions. Examples of quadruped robots of the mammal-type include Spot[1], MIT Cheetah 3[2], Mini Cheetah[3], and ANYmal[4]. Examples of the reptile-type include TITAN-XI[5], TITAN-XIII[6], SILO4[7], and ALPHRED[8]. Examples of hexapod robots with a mammal-type configuration include the Adaptive Suspension Vehicle (ASV) [9] and The Walking Forest Machine developed by John Deere, and those with a reptile-type configuration include COMET-IV[10], DLR-Crawler[11], RiSE V2[12], and LAURON V[13]. Many of the newly developed quadruped robots have a mammal-type configuration, and most of the hexapod robots have a reptile-type configuration. However, few studies have quantitatively compared the performance of robots in each configuration.

Our research group has conducted several studies on the relationship between the configuration of multi-legged robots and their energy efficiency. Hirose and Umetani compared the energy efficiency of two quadruped robot configurations [14]. However, in that study, the robots with 2-DOF leg mechanisms were classified into two configurations according to them body height while walking, and therefore, the definition by 3-DOF leg mechanisms is more meaningful because it corresponds to many of the recent multi-legged robot configurations.

Arikawa and Hirose proposed that in order to improve the energy efficiency of walking robots, it is important to achieve

gravitationally decoupled actuation (GDA) [15]. GDA is a state in which the actuators that support the body weight are separated from the actuators that generate the speed necessary for walking, thereby preventing the actuators from acting as a brake and generating negative power. They have shown that walking with legs spread sideways in the reptile-type configuration can achieve GDA and improve energy efficiency. However, a direct comparison with the mammal-type configuration was not made.

Sanz-Merodio et al. developed a hexapod robot (SILO6) that can utilize both leg configurations through a manual change in the orientation of the legs and compared the energy consumption of both configurations during the walking cycle [16]. In both simulations and experiments on actual machines, the results showed that the mammal-type configuration is more energy efficient. However, in that study, parameters such as body height and foot trajectory were fixed. Therefore, it is not clear how the energy efficiency changes when the walking posture changes for each leg configuration.

When using a multi-legged robot on an unstable foothold with severe unevenness, the points where the feet touch the ground are limited, and it is not always possible to walk in a posture that minimizes the energy consumption. Thus, it is also important to be able to reduce the energy consumption while walking in various postures.

Sanz-Merodio et al. also showed that the mammal-type configuration consumes less energy when the robot walks in an oblique direction. This result contradicts the general idea that the reptile-type configuration has superior mobility in all directions as a result of each leg mechanism being able to move point-symmetrically with respect to the center of rotation of the joint closest to the body. Therefore, it is necessary to verify the energy consumption when capturing various foot trajectories, even when the robot walks diagonally or sideways.

This study aims to conduct a detailed comparison of the power consumed by multi-legged robots during static walking for mammal-type and reptile-type leg configurations. We focus on robots that consist of three joints connected in series and are rotated by electromagnetic motors, which is a common multi-legged robot configuration. We investigate the results after varying certain parameters, such as body height, foot trajectory, payload, and reduction ratio of the joints.

In our analysis, quasi-static motion is assumed, and the mass of the legs is assumed to be negligible. In other words, the kinetic effect is not considered, and only static walking is subjected to the analysis. Consequently, it is difficult to apply the results of this analysis to robots that walk under high-speed leg movement. By contrast, in the case of multi-legged robots working on uneven terrain, such as construction sites or disaster areas, safety is the top priority, and therefore, static walking, which has high stability, is the gait that should be realized first. Accordingly, we verify static walking first as the most basic knowledge.

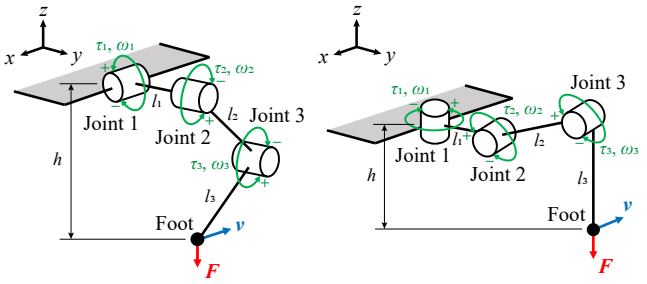

(a) Mammal-type (b) Reptile-type

Fig. 2. Model of the leg mechanism.

II. CONDITIONS FOR ANALYSIS OF POWER CONSUMPTION

A. Modeling of the Leg Mechanism

In this study, we calculate the power consumption of a multi-legged robot, the legs of which consist of 3-DOF serial links. As shown in Fig. 1, the x-axis is defined as the direction of travel (roll axis), the z-axis as the vertical direction (yaw axis), and the y-axis as the direction perpendicular to these (pitch axis). The three joints are defined as Joint 1, 2, and 3 in order of increasing distance from the body. The directions of rotation of the joints in each configuration are defined (in the same order as the joints) as roll, pitch, and pitch in the mammal-type configuration, and yaw, roll, and roll in the reptile-type configuration. The direction of joint bending is defined such that Joint 3 is oriented in the negative direction of the x-axis in the mammal-type configuration, and oriented so that it projects outward in the reptile-type configuration.

The analysis of the power consumption was performed on a model with one extracted leg, as shown in Fig. 2. Therefore, the results of this analysis do not depend on the number of legs. The lengths of the links connecting each joint are denoted as $l_1,\ l_2,\ l_3$. In addition, h is the body height, defined as the vertical distance from Joint 1 to the foot. The angular velocities of each joint are defined as $\omega_1,\ \omega_2,\ \omega_3$, and the output torques of each joint are defined as $\tau_1,\ \tau_2,\ \tau_3$. The output at these joints generates a force $\boldsymbol{F}$ and velocity $\boldsymbol{v}$ at the foot. In this study, static walking, for which the power consumption can be calculated using quasi-static analysis, was considered, and the mass of the leg was assumed to be negligible. Considering this condition, the leg mechanism consumes energy only during the stance phase. To simplify the calculation, the body height h, foot force $\boldsymbol{F}$, and foot velocity $\boldsymbol{v}$ were assumed to be constant during the stance phase. The foot force is balanced by the floor reaction force due to the weight of the robot. We investigated the power consumption when the robot traveled in the x direction, the y direction, and a diagonal direction 45 degrees from the x- and y-axes.

Each parameter was determined by referring to the corresponding value of the quadruped robot TITAN-XIII [6] and equalizing the lengths of l_2 and l_3 such that they would not be unnatural as a mammal-type configuration, as shown in

TABLE I

ASSUMED PARAMETERS OF THE LEG MECHANISM.

Length of the links	l_1	50 mm
	l_2	175 mm
	l_3	175 mm
Body Height	h	125, 225 mm
Foot force	F	24.5 N
Foot velocity	v	0.5 m/s

TABLE II

SPECIFICATIONS OF THE MOTOR USED FOR THE LEG MECHANISM.

Rated output	28 W
Maximum continuous torque	22.48 mNm
No load speed	13300 rpm
Torque constant K_t	19.25 mNm/A
Terminal resistance phase to phase R	2.182 Ω

Table I. Because a raised posture is common for mammal-type robots and a lowered posture is common for reptile-type robots, two values for the body height, $h = 125$ mm and 225 mm, were considered. All joints were driven by the brushless DC motor FX1206-11 manufactured by Nippou Denki, as in TITAN-XIII[6]. Its specifications are shown in Table II. The reduction ratio of the joints was set to $150:1$ for all joints.

B. Power Consumption Calculation Method

From the foot velocity $\boldsymbol{v}$ and the foot force $\boldsymbol{F}$, the angular velocity $\boldsymbol{\omega} = (\omega_1, \omega_2, \omega_3)^T$ and the output torque $\boldsymbol{\tau} = (\tau_1, \tau_2, \tau_3)^T$ of each joint can be calculated using the Jacobian matrix $\boldsymbol{J}$ as follows:

$$\boldsymbol{\omega} = \boldsymbol{J}^{-1}\boldsymbol{v}, \tag{1}$$

$$\boldsymbol{\tau} = \boldsymbol{J}^{T}\boldsymbol{F}. \tag{2}$$

The torque constant of the motor is denoted as K_t, the resistance between terminals is denoted as R, and the reduction ratio of the i-th joint is denoted as ξ_i. Because a quasi-static analysis was performed, the power consumption P can be obtained as follows (ignoring the term that arises due to the time change of the current):

$$P = \sum_{i=1}^{3} \left\{ \alpha_i \tau_i \omega_i + \frac{R}{{K_t}^2} \left(\frac{\tau_i}{\xi_i} \right)^2 \right\}, \tag{3}$$

$$\alpha_i = \begin{cases} 1 & (\tau_i \omega_i \geq 0) \\ 0 & (\tau_i \omega_i < 0) \end{cases}. \tag{4}$$

The first term of (3) represents the power consumed by the mechanical work of the joints, and the second term represents the power consumed by the heat loss in the motors. Assuming the robot is not equipped with a regenerative system, the mechanical power consumption is included in the calculation only when it is positive, as indicated by (4).

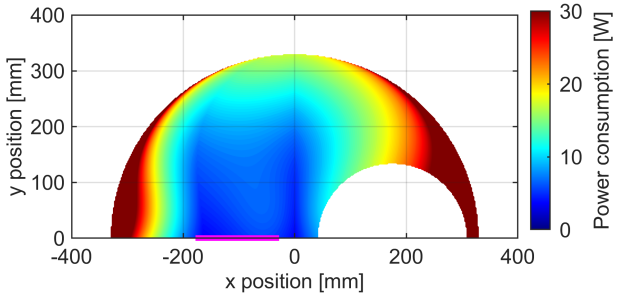

Fig. 3. Total power consumption at each foot position when walking in the x direction in the mammal-type configuration. ($h = 125$ mm)

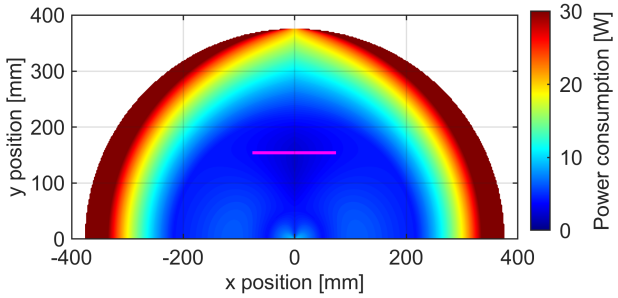

Fig. 4. Total power consumption at each foot position when walking in the x direction in the reptile-type configuration. ($h = 125$ mm)

III. ANALYSIS RESULTS

A. Power Consumption when Walking Forward

1) Relationship between foot position and power consumption: We calculated the power consumed by passing through the foot position that was reachable at the specified body height condition with a foot velocity of $v = 0.5$ m/s, and represented the results in distribution diagrams. In this way, it became clear what foot trajectory should be selected to reduce the power consumption while walking. For the case in which the robot walks forward in the x direction with a body height of $h = 125$ mm, the result for the mammal-type configuration is shown in Fig. 3 and the result for the reptile-type configuration is shown in Fig. 4. For the case of walking forward with a body height of $h = 225$ mm, the result for the mammal-type configuration is shown in Fig. 5 and the result for the reptile-type configuration is shown in Fig. 6. The results shown here were calculated for the left leg, but the same results were obtained for the right leg. The origin of the xy coordinates of the graph was at Joint 1, and the power consumption was calculated for the range of $y \geq 0$ mm, that is, outside the body. If the z-coordinate of Joint 3 is smaller than that of the foot, the joint comes into contact with the ground. In that case, the calculation was not performed as it was out of the range of motion. In the reptile-type configuration, the position where the foot comes to the origin is the singular point, hence, the foot cannot actually pass through this point.

In both configurations, when the body height is lowered, the range of motion of the foot becomes wider toward the

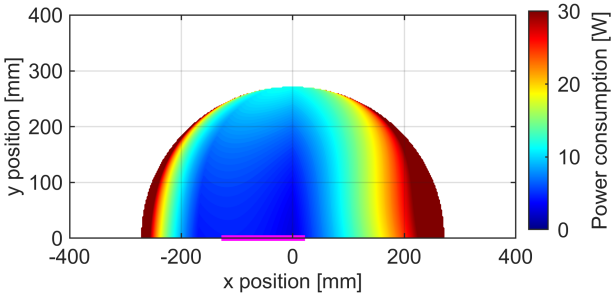

Fig. 5. Total power consumption at each foot position when walking in the x direction in the mammal-type configuration. ($h = 225$ mm)

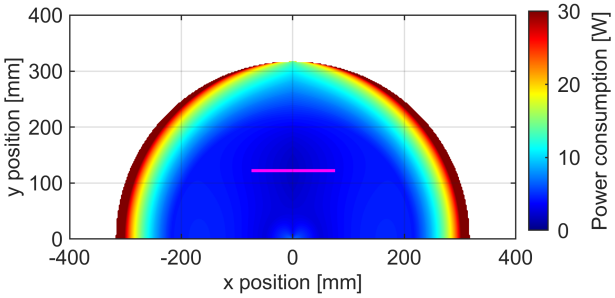

Fig. 6. Total power consumption at each foot position when walking in the x direction in the reptile-type configuration. ($h = 225$ mm)

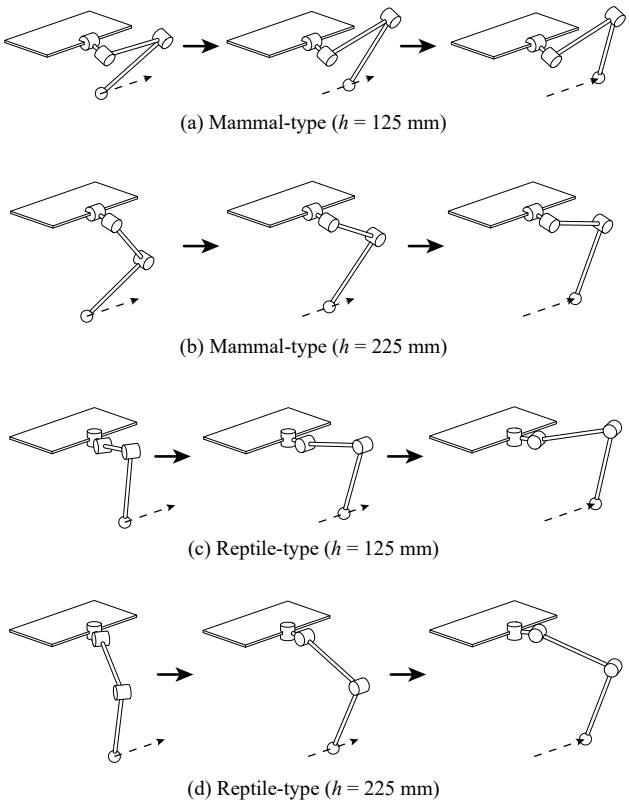

Fig. 7. Postures of the leg mechanism when walking through the foot trajectory that minimizes power consumption.

outside, but the size of the dark blue region, which consumes less power, does not change significantly. The results of these graphs show that regardless of body height, the reptile-type configuration consumes less power over a wider range of foot positions. Therefore, the reptile-type configuration is expected to reduce the power consumption even when its posture is restricted because the points that can be grounded are limited due to the rough ground condition.

Furthermore, the pink line in each graph shows the trajectory that minimizes the energy consumption per step when the stride is 150 mm. For reference, the postures of the leg mechanism when walking with the foot passing through these trajectories are shown in Fig. 7. In the mammal-type configuration, the power consumption is minimized on the straight line represented by $y = 0$ mm (closest to the body), and in the reptile-type configuration, it is minimized at some distance in the y direction from Joint 1. This foot trajectory is generally consistent with the walking posture that is often observed in actual multi-legged robots. The mammal-type posture has the advantage of reducing the width of the robot so that it can enter into narrow areas, while the reptile-type posture has the advantage of a wider support polygon for more stable walking.

We also calculated the mechanical power consumption and the power consumption due to the heat loss in the motors at each foot position for the mammal-type configuration with a body height of $h = 225$ mm and the reptile-type configuration with a body height of $h = 125$ mm. The mechanical power consumption for the mammal-type configuration is shown in Fig. 8, and the result for the reptile-type configuration is shown in Fig. 9. The heat loss for the mammal-type configuration is shown in Fig. 10, and the result for the reptile-type configuration is shown in Fig. 11.

The power consumed by mechanical work is particularly small in the mammal-type configuration near the lines $x = 0$ mm and $x = -165$ mm. In the reptile-type configuration, the mechanical power consumption is small near the line $x = 0$ mm and the circumference of the circle of radius 220 mm centered at the origin. In these regions, the work performed by each motor is very small because the motors that produce torque are separated from the motors that produce angular velocity, establishing GDA [15]. Comparing Figs. 8 and 9, we can see that the reptile-type configuration consumes less power over a wider range of foot positions. In addition, the area of low power consumption extends along the x-axis, which is the same as the direction of travel, and near the straight line $y = 220$ mm. Thus, if the foot is moved within this area, the energy consumption is reduced for the entire walking trajectory.

Figs. 10 and 11 indicate that the power consumption due to the heat loss is also smaller over a wider range of foot positions for the reptile-type configuration. In the mammal-type configuration, the foot position where the heat loss is particularly small is near the point $(x, y) = (-70, 0)$ [mm], whereas in the reptile-type configuration, it is near the circumference of the circle with radius 140 mm centered on the origin.

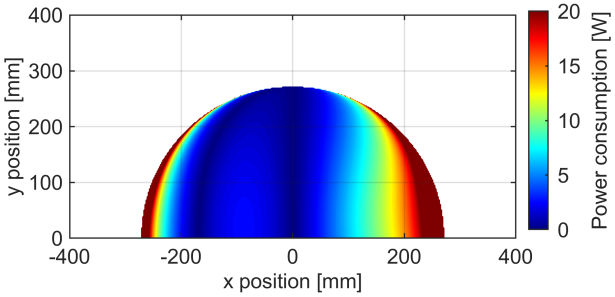

Fig. 8. Mechanical power consumption at each foot position when walking in the x direction in the mammal-type configuration. ($h = 225$ mm)

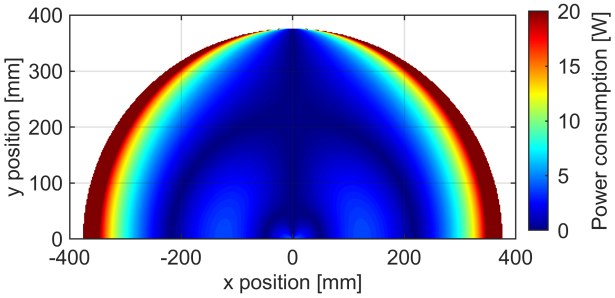

Fig. 9. Mechanical power consumption at each foot position when walking in the x direction in the reptile-type configuration. ($h = 125$ mm)

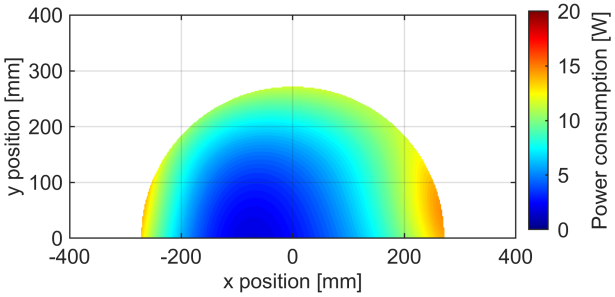

Fig. 10. Heat loss at each foot position when walking in the x direction in the mammal-type configuration. ($h = 225$ mm)

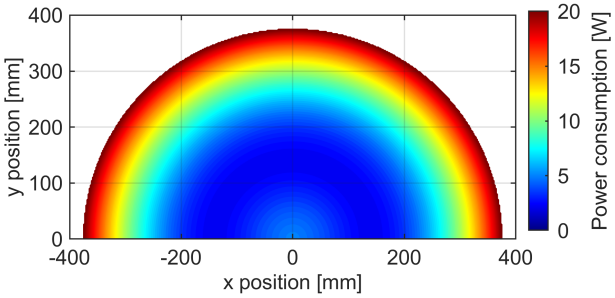

Fig. 11. Heat loss at each foot position when walking in the x direction in the reptile-type configuration. ($h = 125$ mm)

2) Relationship between body height, load magnitude, and power consumption: To investigate the relationship between the body height and the power consumption during walking, we derived the foot trajectory that minimizes the energy consumption per step for each body height using the same procedure to draw the pink lines in Figs. 3–6. We calculated the time average of the power consumption when following that trajectory at a constant speed $v = 0.5$ m/s. Fig. 12(a) shows the results for each leg configuration. To investigate the effect of changing the magnitude of the load, the results of the case in which a load of 5 kg was added to each leg are shown in Fig. 12(b). However, when the body height is lowered, there are certain postures in which the joints are very close to the ground, which is not possible in an actual robot. Therefore, the trajectory that consumed the least amount of energy was determined for the condition that each joint was always higher than 50 mm off the ground. In Fig. 12, the time averages of the mechanical power consumption and the heat loss when the foot follows the trajectory that minimizes the energy consumption are shown as broken and dotted lines, respectively. At the point where the power consumption changes discontinuously, the position of the walking trajectory where the total power consumption is minimum is shifted.

Fig. 12 demonstrates that for both leg configurations, the total power consumption is at a local maximum when the body height is close to 150 mm. However, for the mammal-type configuration, when the body height is lowered considerably, the range of foot motions is limited, and the robot is forced to choose a foot trajectory that consumes more power. In light of this, it is desirable to increase the body height in a mammal-type configuration in order to reduce the power consumed while walking. In contrast, in the reptile-type configuration, whether the body height is raised or lowered, the power consumption during walking can be reduced. Therefore, it is desirable to lower the body height in the reptile-type configuration, especially considering the wide range of motion of the foot and the difficulty of falling.

Comparing the magnitude of the power consumption for each leg configuration, it is clear that the total power consumption is smaller for the reptile-type configuration whether or not there is a payload. In addition, because the magnitude of the heat loss is not significantly different between the two leg configurations, the difference in the total power consumption is due to the difference in the magnitude of the mechanical power consumption. The ratio of the heat loss to the mechanical power consumption varies with the magnitude of the load; when a payload is added, the heat loss accounts for a larger percentage of the total power consumption. Then, as the magnitude of the heat loss is not significantly different between the two leg configurations, the difference in the total power consumption becomes small. The results suggest that the difference in the total power consumption between the two leg configurations becomes small when the heat loss is increased by factors such as an increased load, a decreased reduction ratio of the joint, or a motor that generates a large amount of heat due to the large resistance between terminals relative to the torque constant. On the contrary, if the ratio of the mechanical power consumption increases due to factors such as an

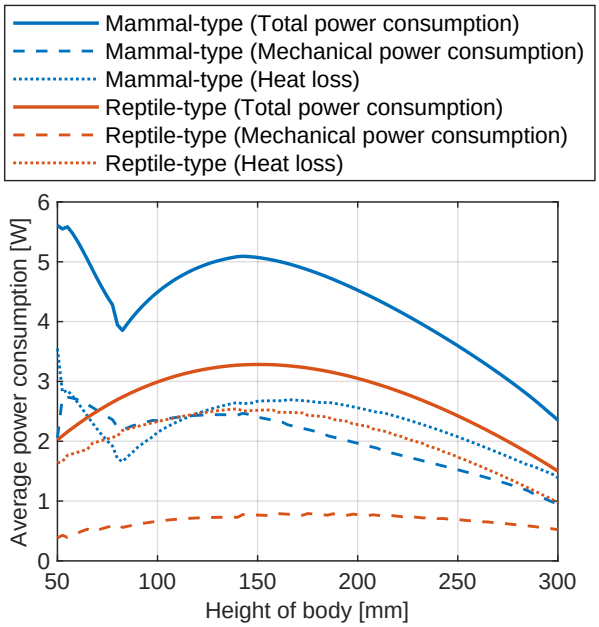

(a) without payload

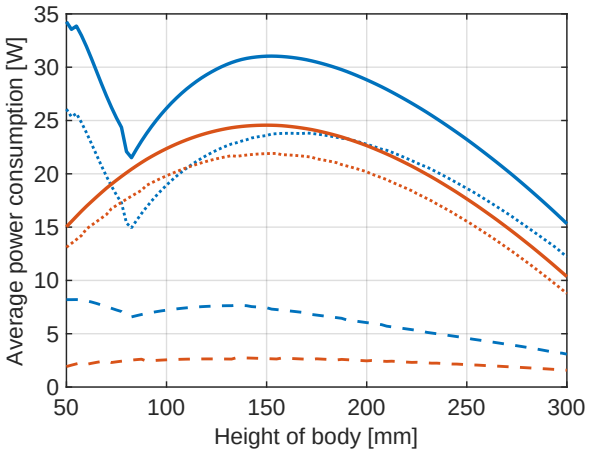

(b) with 5 kg payload per leg

Fig. 12. Relationship between body height and average power consumption for the trajectory that minimizes energy consumption per step.

increased walking speed or a reduction of the mass of the robot, the difference in the total power consumption between the two leg configurations increases, and the reptile-type configuration becomes more advantageous in terms of power consumption.

In the study by Sanz-Merodio et al., the walking speed of the robot was small (approximately 0.18 m/s) and its mass was relatively large (44.34 kg) compared to the length of the legs, which increased the percentage of the heat loss [16]. As can be seen from Fig. 12, which configuration results in a higher heat loss depends on conditions such as body height. However, they compared two configurations by fixing the body height and walking trajectory, which may have resulted in a lower power consumption in the mammal-type configuration.

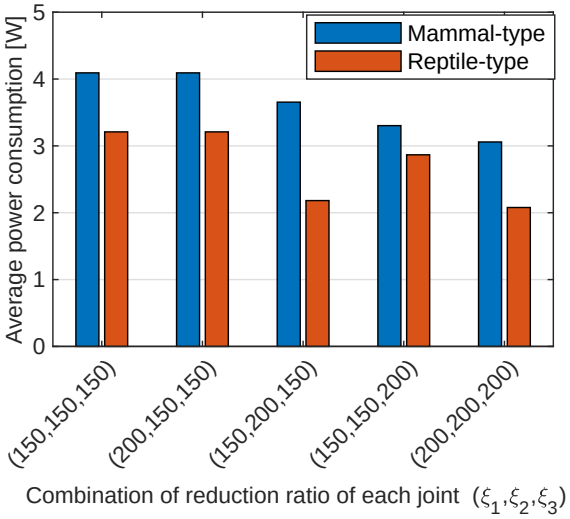

Fig. 13. Relationship between reduction ratio of each joint and average power consumption in the trajectory that minimizes energy consumption per step. The reduction ratio of the i-th joint from the body is denoted as ξ_i.

3) Relationship between reduction ratio of each joint and power consumption: From the discussion in Section III-A.2, it is expected that as the reduction ratio of the joint is increased, the total power consumption is decreased due to the smaller heat loss, and the difference in the power consumption between the two leg configurations increases. To investigate how the power consumption changes when the reduction ratio of each joint is assigned a non-uniform value, we conducted an analysis to calculate the power consumption when the reduction ratio of only one joint is increased. An analysis was performed for each leg configuration, with a body height h of 225 mm for the mammal-type configuration and 125 mm for the reptile-type configuration. The reduction ratio of each joint was set to $150:1$ or $200:1$. We calculated the time average of the power consumption when the robot walks in the trajectory that minimizes the energy consumption per step, similar to the method used to obtain the results in Fig. 12. The results are shown in Fig. 13.

Comparing the case in which all the reduction ratios are $150:1$ and the case in which all the reduction ratios are $200:1$, we confirmed that when the reduction ratios are high, the total power consumption becomes small and the difference in the power consumed by each leg configuration becomes large.

When only the reduction ratio of Joint 1 is changed, the magnitude of the power consumption does not change. This is because the motor driving Joint 1 does not operate at all when the multi-legged robot in the mammal-type configuration walks forward following the exact trajectory of $y = 0$ mm. In the reptile-type configuration, the torque due to the vertical load generated by the foot does not act on Joint 1.

The power consumption is greatly reduced when the reduction ratio is increased in Joint 3 for the mammal-type configuration and in Joint 2 for the reptile-type configuration.

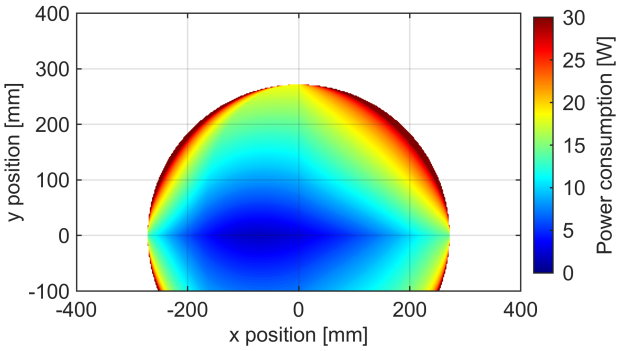

Fig. 14. Total power consumption at each foot position when walking in the y direction in the mammal-type configuration. ($h = 225$ mm)

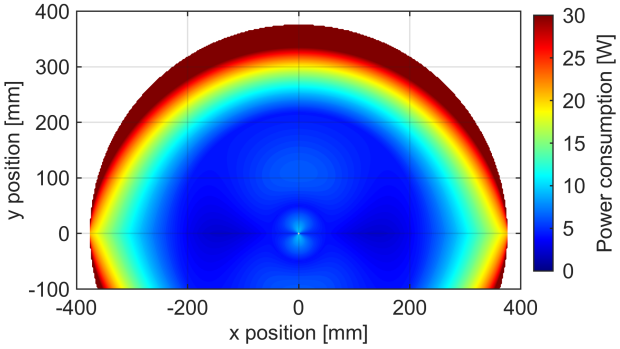

Fig. 15. Total power consumption at each foot position when walking in the y direction in the reptile-type configuration. ($h = 125$ mm)

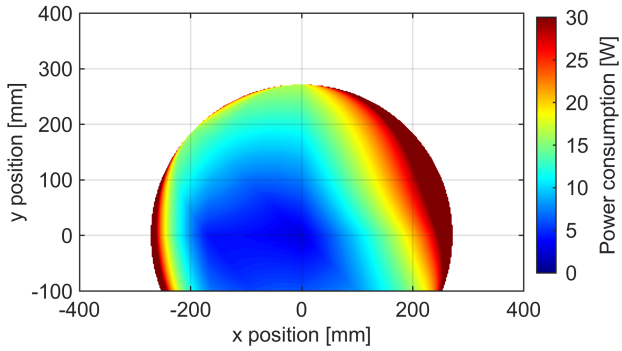

Fig. 16. Total power consumption at each foot position when walking in the direction of the vector $(x, y)^T = (1, 1)^T$ in the mammal-type configuration. ($h = 225$ mm)

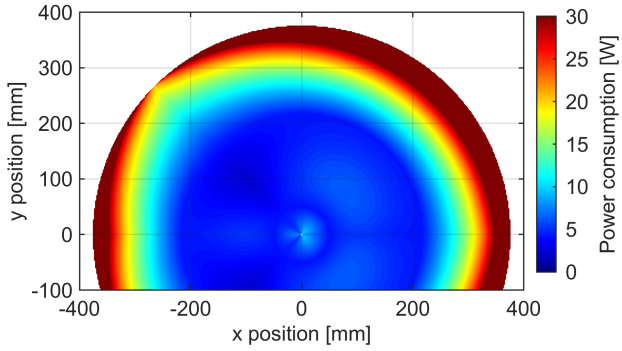

Fig. 17. Total power consumption at each foot position when walking in the direction of the vector $(x, y)^T = (1, 1)^T$ in the reptile-type configuration. ($h = 125$ mm)

The change in the power consumption is particularly large when the reduction ratio of Joint 2 is increased in the reptile-type configuration, which indicates that the motor driving Joint 2 bears much of the torque required to support its own weight and generates most of the heat loss during the walking motion. When designing a multi-legged robot, increasing the reduction ratio of the motor that generates such a large amount of heat loss can improve energy efficiency while maintaining the maximum walking speed as high as possible. This effect is particularly noticeable in the reptile-type configuration, in which the roles of the motors that produce torque and those that produce angular velocity are clearly separated.

B. Power Consumption when Walking Sideways or Diagonally

To investigate the power consumption when the robot walks in a direction other than the forward direction, we calculated the power consumption when it walked sideways: in the direction of the y-axis in Fig. 1, and in the direction of $(x, y)^T = (1, 1)^T$ (the diagonal direction of 45 degrees from the x- and y-axes). The results were expressed in the form of distribution diagrams showing the power consumed by passing through each foot position within the range of motion at a constant foot velocity of $v = 0.5$ m/s. To consider movement in the y direction, calculations were made up to a range of $y \geq -100$ mm. The body height h is 225 mm for the mammal-type configuration and 125 mm for the reptile-type configuration. The power consumption when walking sideways for the mammal-type configuration is shown in Fig. 14, and that of the reptile-type configuration is shown in Fig. 15. The power consumption when walking diagonally for the mammal-type configuration is shown in Fig. 16, and that of the reptile-type configuration is shown in Fig. 17.

Figs. 15 and 17 suggest that the results for the reptile-type configuration are obtained by rotating Fig. 4 around the origin, which is the result for walking forward. The power consumption in the reptile-type configuration remains small over a wide range of foot positions, just as when walking forward. In contrast, for the mammal-type configuration, the power consumption is larger in the area where the y-coordinate is larger and farther from the body. Unlike when walking forward, in walking sideways or diagonally the foot needs to pass through a trajectory that is farther from the body, which increases the power consumption per step. Therefore, the reptile-type configuration consumes less power when walking in various directions. This feature suggests that a robot with a reptile-type configuration consumes less power even when it needs to meander because of surrounding obstacles or rough ground conditions.

IV. CONCLUSIONS

In this study, we compared the power consumed during static walking for mammal-type and reptile-type leg configurations, varying parameters such as body height, foot trajectory, payload, and reduction ratio of the joints. The results of the analysis revealed the following properties:

1) Regardless of the direction of walking, the reptile-type configuration consumed less power while walking in a wide range of foot positions.
2) Lowering the body height of the reptile-type configuration simultaneously reduced the power consumption, improved stability, and expanded the range of foot positions.
3) In the reptile-type configuration, by increasing the reduction ratio of the second joint from the body, the power consumption was reduced without significantly reducing the maximum walking speed.

These results indicate that the reptile-type configuration is superior in terms of the power consumption during static walking. Multi-legged robots with a reptile-type configuration are considered to be suitable for situations where the terrain is rough and a stable power supply is not expected, such as at disaster areas, due to their ability to reduce the power consumption even in various walking postures. In addition, we found that the difference in the power consumption between the two leg configurations becomes smaller when the effect of the heat loss in the motors becomes large.

These findings are not necessarily applicable to the case of high-speed walking robots. However, the results of this study may be applicable to situations where stable walking, even at low speed, is the primary requirement.

In future work, we will compare the leg configurations taking into account the magnitude and direction of the force applied to the foot, and conduct a dynamic analysis. We will also quantitatively compare the maximum speed and force that can be produced by multi-legged robots under each leg configuration.

REFERENCES

[1] "Spot® - The Agile Mobile Robot | Boston Dynamics," [Online]. Available: https://www.bostondynamics.com/products/spot. Accessed: Nov. 12, 2021.

[2] G. Bledt , M. J. Powell, B. Katz, J. Di Carlo, P. M. Wensing, and S. Kim, "MIT Cheetah 3 : Design and Control of a Robust, Dynamic Quadruped Robot," in *2018 IEEE/RSJ International Conference on Intelligent Robots and Systems (IROS)*, pp. 2245–2252, 2018.

[3] B. Katz, J. D. Carlo and S. Kim, "Mini Cheetah: A Platform for Pushing the Limits of Dynamic Quadruped Control," in *2019 International Conference on Robotics and Automation (ICRA)*, pp. 6295–6301, 2019.

[4] M. Hutter et al., "ANYmal - a highly mobile and dynamic quadrupedal robot," in *2016 IEEE/RSJ International Conference on Intelligent Robots and Systems (IROS)*, pp. 38–44, 2016.

[5] R. Hodoshima, T. Doi, Y. Fukuda, S. Hirose, T. Okamoto and J. Mori, "Development of TITAN XI: a quadruped walking robot to work on slopes," in *2004 IEEE/RSJ International Conference on Intelligent Robots and Systems (IROS)*, pp. 792–797, 2004.

[6] S. Kitano, S. Hirose, A. Horigome and G. Endo, "TITAN-XIII : sprawling-type quadruped robot with ability of fast and energy-efficient walking," *ROBOMECH Journal*, Vol. 3, No. 1, pp. 1–16, 2016.

[7] P. G. De Santos, J. A. Galvez, J. Estremera, and E. Garcia, "SILO4: a true walking robot for the comparative study of walking machine techniques," *IEEE Robotics and Automation Magazine*, Vol. 10, No. 4, pp. 23–32, 2003.

[8] J. Hooks, M. S. Ahn, J. Yu, X. Zhang, T. Zhu, H. Chae, and D. Hong, "ALPHRED: A Multi-Modal Operations Quadruped Robot for Package Delivery Applications," *IEEE Robotics and Automation Letters*, Vol. 5, No. 4, pp. 5409–5416, 2020.

[9] K. Waldron and R. McGhee, "The adaptive suspension vehicle," *IEEE Control Systems Magazine*, Vol. 6, No. 6, pp. 7–12, 1986.

[10] A. Irawan and K. Nonami, "Compliant Walking Control for Hydraulic Driven Hexapod Robot on Rough Terrain," *Journal of Robotics and Mechatronics*, Vol. 23, No. 1, pp. 149–162, 2011.

[11] M. Gorner et al., "The DLR-Crawler: A testbed for actively compliant hexapod walking based on the fingers of DLR-Hand II," in *2008 IEEE/RSJ International Conference on Intelligent Robots and Systems (IROS)*, pp. 1525–1531, 2018.

[12] M. J. Spenko, G. C. Haynes, J. A. Saunders, M. R. Cutkosky, A. A. Rizzi, R. J. Full, and D. E. Koditschek, "Biologically inspired climbing with a hexapedal robot," Vol. 25, Issue 4–5, pp. 223–242, 2008.

[13] A. Roennau, G. Heppner, M. Nowicki and R. Dillmann, "LAURON V: A versatile six-legged walking robot with advanced maneuverability," in *2014 IEEE/ASME International Conference on Advanced Intelligent Mechatronics*, pp. 82–87, 2014.

[14] S. Hirose and Y. Umetani, "Some Considerations on a Feasible Walking Mechanism as a Terrain Vehicle," in *3rd CISM-IFToMM International Symposium on Theory and Practice of Robots and Manipulators*, pp. 357–375, 1978.

[15] K. Arikawa and S. Hirose, "Mechanical design of walking machines," *Philosophical Transactions of the Royal Society A*, Vol. 365, pp. 171–183, 2007.

[16] D. Sanz-Merodio, E. Garcia and P. Gonzales-de-Santos, "Analyzing energy-efficient configurations in hexapod robots for demining applications," *Industrial Robot*, Vol. 39, No. 4, pp. 357–364, 2012.